JOURNAL OF AGRICULTURAL AND FOOD CHEMISTRY

Effect of Temperature and Glassy States on the Molecular Mobility of Solutes in Frozen Tuna Muscle As Studied by Electron Spin Resonance Spectroscopy with Spin Probe Detection

VIBEKE ORLIEN, MOGENS L. ANDERSEN,* SAARA JOUHTIMÄKI, JENS RISBO, AND LEIF H. SKIBSTED

Food Chemistry, Department of Dairy and Food Science, Royal Veterinary and Agricultural University, Rolighedsvej 30, DK-1958 Frederiksberg C, Denmark

The mobility of solutes in frozen food systems (tuna muscle, sarcoplasmic protein fraction of tuna muscle, and carbohydrate−water) has been studied using the temperature dependence of the shape of electron spin resonance (ESR) spectra of the spin probe 4-hydroxy-2,2,6,6-tetramethylpiperidine-N-oxyl (TEMPOL). The spin probe was incorporated into the tuna meat from an aqueous solution of TEMPOL or by contact with a layer of TEMPOL crystals. The melting/freezing of freeze-concentrated solutes in frozen tuna meat was observed to take place over a range of temperatures from −25 to −10 °C. Lower temperatures gave ESR powder spectra due to the decreased mobility of the spin probe, and the temperature dependence of the mobility of the spin probe did not show abrupt changes at the glass transition temperatures of the systems. The mobility of nonglass forming solutes is concluded to be decoupled from the glass forming components. Similar behavior was also observed for TEMPOL in frozen, aqueous carbohydrate systems. The temperature dependence of the mobility of TEMPOL in the frozen systems was analyzed using the Arrhenius equation, and the logarithm of the Arrhenius preexponential factor τ_a was found to be linearly correlated with the activation energy for all of the tuna and carbohydrate samples, indicating a common molecular mechanism for the observed mobility of TEMPOL in all of the systems. The linear correlation also suggests that the observed mobility of TEMPOL in the frozen aqueous systems is dominated by enthalpy−entropy compensation effects, where the mobility of TEMPOL is thermodynamically strongly coupled to the closest surrounding molecules.

KEYWORDS: Frozen tuna; ESR; solute mobility; glass transition; melting

INTRODUCTION

Freezing is a common method for long-term storage of foods, and the subzero temperatures are assumed to suppress the deteriorating reactions, primarily by thermodynamic restrain on the reaction rates. However, storage of food at the normal freezing temperature (−18 °C) does not completely hinder the degradation of quality, and deteriorative reactions proceed, albeit very slowly, at temperatures below the freezing point of the aqueous phase. Foods that are susceptible to oxidation, such as fish meat, have been reported to degrade during frozen storage (*1*−*3*).

The macroscopic properties of frozen systems have been studied intensively, mainly by differential scanning calorimetry (DSC), often leading to the construction of state diagrams that summarize the thermodynamic characteristics such as melting temperatures and the glass transition temperatures, T_g (*4*−*7*). Particularly the temperature of formation of the maximally freeze-concentrated glass (T_g') is expected to be of crucial importance for the food stability in relation to storage temperature. It has been suggested that improved long-term storage stability of food can be achieved by storing food in a frozen amorphous glassy state, where the molecules form a nonperiodic and nonsymmetric network presumably resulting in an extremely high viscosity and thus immobilized molecules. Because of this very limited molecular motion, a food product in a glassy state is assumed not to deteriorate during storage (*8*−*12*). However, the possibility that transition of the food system into a glassy state may not be sufficient to limit molecular motions has recently been discussed (*13*−*15*).

Information about structural and dynamic properties at a microscopic (molecular) level is becoming of increasing interest in the study of molecular motions in frozen biological systems. Characterization of molecular mobility at subzero temperatures of compounds similar in sizes to compounds that are involved in degradation reactions is expected to give a better understand-

* To whom correspondence should be addressed. Tel: +45 3528 3262. Fax: +45 3528 3344. E-mail: mola@kvl.dk.

10.1021/jf034931g CCC: $27.50
Published on Web 03/19/2004

ing of degradation of frozen foods and of the hypothetical positive effect of the glassy state. The mobility of a paramagnetic guest molecule (spin probe) introduced into the glassy system under investigation in a system above and below the glass transition temperature can be studied by electron spin resonance (ESR) spectroscopy, from which the rotational and librational mobility characteristics can be extracted as a function of temperature. In this context, spin probe ESR is particular useful, since the obtained data reflect the mobility of low molecular weight solutes. Several applications of spin probe ESR in glassy systems have been described in the literature (*16*−*21*), and recently, the mobility of solutes in frozen pork was successfully studied by this technique (*22*).

Recently, the ice formation and glass formation in frozen tuna muscle have been characterized (*7*, *23*), and the supplemented state diagram for frozen tuna was constructed based on DSC measurements (*7*). In the present paper, the effect of temperature and the formation of a glassy state on the molecular mobility in frozen tuna fish is studied using the spin probe technique. This includes a systematic study of the molecular mobility of solutes in tuna muscle, in the protein fraction of tuna muscle responsible for the glass formation, in a well-characterized glassy system based on carbohydrates, and in a nonglass forming system. To do this, a nitroxyl spin probe has been incorporated into the respective systems, and ESR spectroscopy was used to monitor the temperature-dependent changes in the mobility of the probe, which are reflected in the pattern of the ESR spectra. This approach provides information about molecular mobility of solutes and glassy states in frozen foods and about the relationship of mobility with the glass transition temperatures, which further is important for an understanding of phenomena such as lipid oxidation and lipolysis that might take place during frozen storage.

MATERIALS AND METHODS

Tuna Samples. Fresh tuna muscle, obtained from a local retailer, was cut into cubes (size 2 cm × 2 cm × 2 cm), and the samples with an incorporated spin probe were prepared in a similar way as described previously for pork (*22*).

Tuna Sample A. A buffered spin probe solution (2.0 mM) was made by dissolving 4-hydroxy-2,2,6,6-tetramethylpiperidine-1-oxyl (TEMPOL; Sigma, St. Louis, MO, used without further purification) in a phthalate buffer (0.1 M and pH 5.8). A cube of tuna muscle was immersed in an equal weight of the buffered spin probe solution overnight at 5 °C.

Tuna Sample B. A cube of tuna muscle was immersed in an equal weight of aqueous solution of the spin probe (2 mM) overnight at 5 °C.

Tuna Sample C. An ethanol solution of TEMPOL (0.02 mM) was spread on a 20 cm^2 glass surface, and the ethanol was gently evaporated, resulting in a thin layer of TEMPOL crystals. A small tuna cube was placed on the crystal layer overnight at 5 °C.

Sarcoplasmic Proteins. The procedure of Brake and Fennema (*24*) was used for isolating the water soluble sarcoplasmic protein fraction from the tuna meat. The isolated sarcoplasmic protein fraction, which may contain low molecular weight salts and sugars, was freeze-dried and rehydrated to 20% dry matter w/w with aqueous spin probe solution (2.0 mM). An aliquot of approximately 3 mg was packed between two plastic layers as described below.

Control Samples. Aliquots of aqueous TEMPOL solution or buffered aqueous TEMPOL solution were packed as described below prior to ESR experiments.

Carbohydrate Samples. Samples were made from sucrose (Merck, Germany), maltooligosaccharide (maltodextrin) with 5, 9, or 18.5 dextrose equivalent (DE) (Cerestar France S. A.), and Milli-Q-water (Millipore Q-Plus, Millipore Corporation, Bedford, MA). Carbohydrates were dissolved in boiling Milli-Q-water with continuous stirring. Sample weights were adjusted afterward by adding appropriate amounts of water to the samples until the water contents of the samples were stable. TEMPOL was mixed directly into the samples, giving a final TEMPOL concentration of 2.3 mM. Carbohydrate systems were prepared as described above for the ESR experiments.

ESR Experiments. First-derivative ESR spectra were recorded on a Bruker ECS 106 X band ESR spectrometer (Bruker, Rheinstetten, Germany) equipped with an ER 4103 TM cavity, a Bruker ER 4121 VT continuos-flow liquid nitrogen temperature controller, and a Dewar insert for flat aqueous cells (Wilmad, Buena, NJ). Prior to the ESR experiments, small slices of the marinated tuna samples (A, B, or C) were placed between two layers of plastic foil (NEN 40 HOB/LLDPE 75, Dansico Flexible, Lyngby, Denmark) (size 1 mm × 1 mm × 1 mm) and sealed with a T300 table sealer. The plastic cells with the tuna or control samples were kept in place inside the Dewar insert by fixing it to a plastic spatula. The measurements were made with the following general settings: microwave power, 0.2 mW; modulation frequency, 100 kHz; modulation amplitude, 1 G; time constant, 647 ms; and conversion time, 647 ms. The samples were inserted at −90 °C, and the temperature was then gradually raised to 0 °C in steps of 5 °C. At each step, an ESR spectrum was recorded.

DSC Measurements. The glass transition temperatures were measured by DSC (DSC 820, Mettler Toledo, Schwerzenbach, Switzerland). The DSC 820 was based on the heat flux principle and cooled with liquid nitrogen. Calibration of heat flow and temperature was performed with indium and zinc as the standard (T_m = 156.6 °C, ΔH_{fus} = 28.5 J/g and T_m = 419.5 °C, ΔH_{fus} = 107.5 J/g, respectively). The low temperature linearity of the calibration was verified with decane (T_m = −29.66 °C) and cyclohexane (T_m = 6.47 °C). Approximately 10 mg of sample was hermetically sealed into 40 μL aluminum DSC crucibles (ME 27331, Mettler Toledo). As reference, an empty sealed aluminum crucible was used. The glass transition of the maximally freeze-concentrated glass, T_g', was measured by using conventional DSC with an annealing procedure and alternating DSC (ADSC). In conventional DSC, the sample was annealed isothermally at a temperature between T_g' and T_m' (the onset of ice melting) for 90−100 min to ensure maximally freeze-concentrated glass and then scanned over an appropriate temperature range with 10 °C/min (*7*). For ADSC, samples were cooled to −100 °C and then subjected to an oscillating heating profile with an underlying heating rate of 1 °C/min, an amplitude of 1 °C, and a time period of 1 min. T_g' was determined as the onset temperature of the transitions that were determined by appropriate tangent construction using the DSC software packages supplied with the instruments.

RESULTS

The spin probe TEMPOL was incorporated into tuna meat by a marinating procedure that has been used previously for pork meat (*22*). The tuna meat was placed in a phthalate buffered solution of TEMPOL, and the spin probe was allowed to diffuse into the meat overnight (sample A). Frozen slices of TEMPOL marinated tuna meat gave typical nitroxyl ESR powder spectra demonstrating the presence of a nitroxyl radical immobilized by trapping in the frozen matrix (**Figure 1**).

The ESR powder spectra of the frozen tuna were studied between −90 and −10 °C. This range of temperatures covers the glass transition zone of tuna meat (−74 to −55 °C), and the tuna was therefore studied in both a freeze concentrated nonglassy state and a frozen glassy state (*7*). The shape of the powder spectra was temperature-dependent, which is caused by changes in the rotational mobility of the spin probe (*25*). The changes in the ESR spectrum were quantified by the observed anisotropic hyperfine coupling constant, A_{zz}', which is given as half the separation between the two outer peaks in the ESR spectrum (*22*) (**Figures 1** and **2**). At low temperatures (from −90 to −65 °C), A_{zz}' was found to level off indicating that the rotational mobility of the TEMPOL spin probe was so slow that it was close to the limit of detection by continuous wave

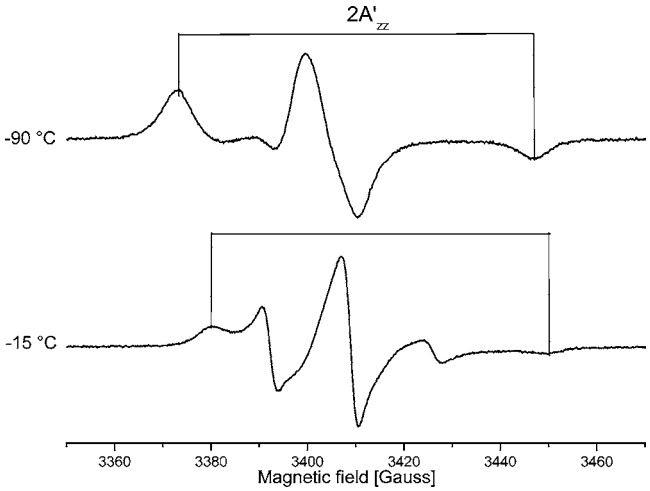

Figure 1. ESR spectra of tuna meat marinated with a buffered TEMPOL solution at −90 and −15 °C. The observed hyperfine coupling constant A_{zz}' was determined as the half of the splitting between the outer two peaks of the powder spectra.

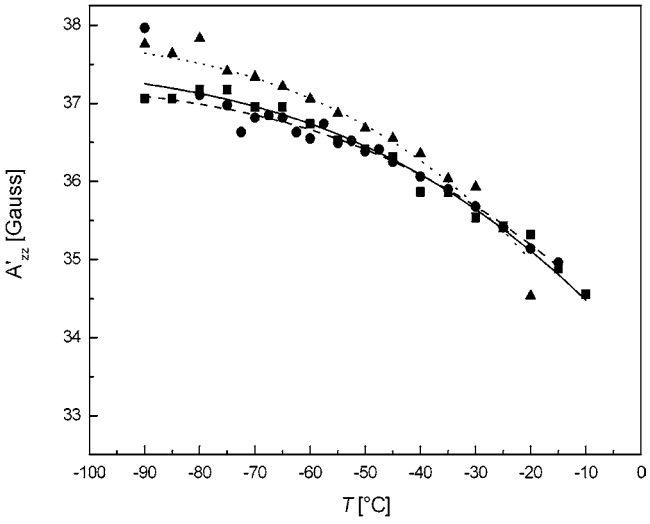

Figure 2. Observed hyperfine coupling constant A_{zz}' as a function of temperature for tuna meat containing TEMPOL. Tuna marinated in a buffered TEMPOL solution (■, —), tuna marinated in a nonbuffered aqueous TEMPOL solution (●, - - -), and tuna where TEMPOL has been absorbed by the meat directly from a layer of TEMPOL crystals (▲, • • •). The lines are the results of the fitting procedure described in the text.

X-band ESR (**Figure 2**) (*26*). Between −65 and −10 °C, a gradual decrease in A_{zz}' as a result of increased mobility of TEMPOL was observed, reflecting a decrease in the viscosity of the frozen matrix. The measured values of A_{zz}' were independent of the direction of the temperature changes. Going from low temperatures to high temperatures gave the same results as changing the temperatures in the opposite direction, demonstrating that the temperature dependence of A_{zz}' is reversible and invariant of whether the sample had been brought to the given measurement temperature from an initial higher or lower temperature.

The powder ESR spectrum of TEMPOL in the tuna sample A changed toward an isotropic three line solution spectrum at temperatures above −25 °C, and above −10 °C, only an isotropic three line solution spectrum was observed. These spectral changes are associated with the melting of ice, and the mixture of a powder spectrum and a three line solution spectra

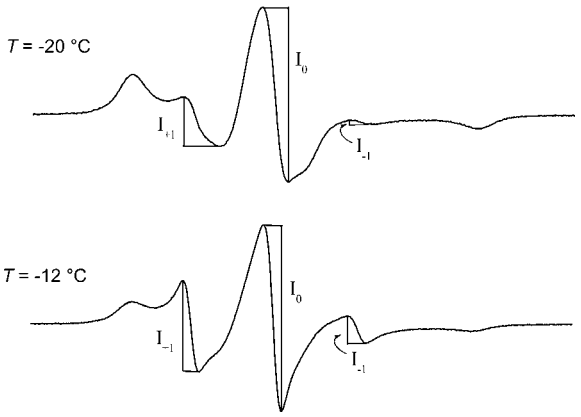

Figure 3. Line heights I_{+1}, I_0, and I_{-1} of mixture spectra of a powder spectrum and an isotropic solution spectrum.

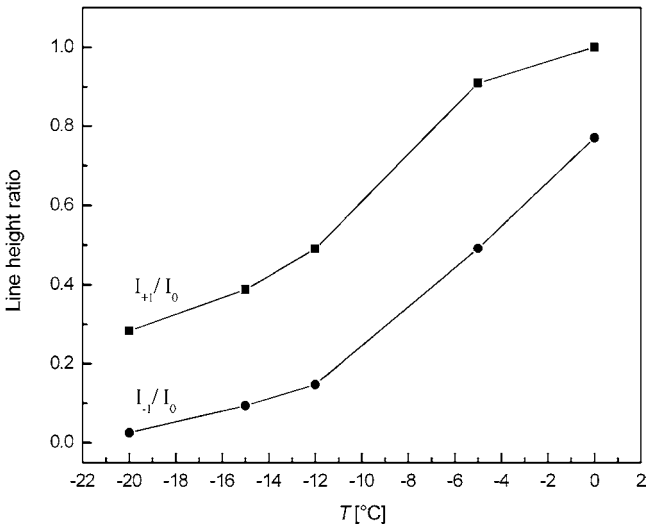

Figure 4. Ratios I_{+1}/I_0 (■) and I_{-1}/I_0 (●) of the mixture spectra of the tuna sample with buffered TEMPOL as a function of temperature.

indicates that the frozen tuna meat in this temperature range consists of a mixture of domains of ice and partially freeze concentrated tuna meat. This is in agreement with DSC experiments, where the melting of ice in this temperature range was observed and the lower boundary for equilibrium ice formation, T_m', was determined to be −29 °C (*7*). The changes in the shape of a nitroxyl powder spectrum toward the shape of an isotropic three line solution were quantified by the ratios I_{+1}/I_0 and I_{-1}/I_0, where I_{+1}, I_0, and I_{-1} are the heights of the isotropic ESR lines and the powder spectrum underneath (**Figure 3**). The ratios of I_{+1}/I_0 and I_{-1}/I_0 increased with the temperature between −20 and 0 °C and approach unity at high temperatures, which reflect a gradual melting of ice domains in this temperature interval (**Figure 4**).

The thermal stability of the frozen tuna at temperatures above −30 °C was investigated by keeping a tuna sample A, which initially had been frozen to −80 °C, at different temperatures (−30, −25, −20, −15, and −12 °C) for 1 h. The shape of the ESR spectra of the tuna sample did not change with time, which was observed as constant values of the ratios I_{+1}/I_0 and I_{-1}/I_0 at each of the temperatures. These experiments led to the conclusion that the samples are in thermal equilibrium under the conditions of the ESR experiments.

Using a buffered TEMPOL solution for marinating the tuna meat could potentially affect the marinated meat either by depleting the meat of solutes that may diffuse into the TEMPOL solution or by the diffusion of buffer into the meat. Two

Table 1. Glass Transition Temperatures, Rigid Limit Hyperfine Coupling Constants, and Arrhenius Activation Parameters for the Rotational Mobility of TEMPOL in Frozen Tuna Systems[a]

sample (symbol)[b]	T_g' (°C)	A_{zz} (Gauss)	E_a (kJ/mol)	log(τ_a)
tuna sample A (■, —)	−74[c]	37.46 ± 0.13	13.8 ± 0.6	−10.55 ± 0.13
tuna sample B (●, - - -)	−74[c]	37.30 ± 0.13	14.6 ± 0.7	−10.66 ± 0.16
tuna sample C (▲, · · ·)	−74[c]	37.84 ± 0.15	15.3 ± 0.5	−10.94 ± 0.11
sarcoplasmic proteins (■, —)	−67[c]	37.09 ± 0.07	28.6 ± 3.0	−13.77 ± 0.73

[a] Errors are reported as the SD. [b] The symbol and line refer to **Figures 2** and **6** (sarcoplasmic proteins). [c] Measured with DSC. From ref *7*.

alternative methods for incorporating the spin probe into the meat were therefore used in order to examine the effect of the TEMPOL containing medium on the final marinated tuna meat. Tuna meat was placed in a nonbuffered aqueous solution of TEMPOL (sample B) or placed on top of a glass surface covered by a thin layer of TEMPOL crystals (sample C) in order to avoid the effect of long-term contact of the meat with a solvent. Both methods gave samples of tuna meat containing TEMPOL, as evidenced by the detection by ESR in slices cut 1 mm from the surface. The freezing behavior of the meat sample was found to be independent of the composition of the TEMPOL solution that was used to introduce the spin probe into the meat. The temperature dependence of A_{zz}' for sample B gave an analogous trend as observed for sample A (**Figure 2**). The incorporation of the spin probe into the meat by absorption directly from TEMPOL crystals, sample C, gave a similar temperature dependency of the A_{zz}' values as for sample A (**Figure 2**).

The temperature dependence of the anisotropic hyperfine coupling constants, A_{zz}', was analyzed by determining the Arrhenius activation parameters for the rotational motion of TEMPOL. The relation between the rotational correlation time, τ_c, of TEMPOL in frozen matrixes and the value of the anisotropic hyperfine coupling constants, A_{zz}', is to a good approximation given by eq 1, where A_{zz} is the rigid limiting value of A_{zz}' (*25*, *27*). The values of the constants $a = 1.09 \times 10^{-9}$ s and $b = -1.05$ in eq 1 are based on a Brownian diffusion model for the rotational mobility.

$$\tau_c = a \times (1 - A_{zz}'/A_{zz})^b \quad (1)$$

The activation energy, E_a, for the rotational mobility of the spin probe was obtained by using an Arrhenius type equation for the temperature dependence of τ_c, eq 2, where τ_a is a temperature-independent preexponential factor (*27*).

$$\tau_c = \tau_a \times \exp(E_a/RT) \quad (2)$$

The combination of eqs 1 and 2 gives eq 3 from which A_{zz} was determined from the anisotropic hyperfine coupling constants, A_{zz}', by fitting as shown in **Figure 2**.

$$A_{zz}' = A_{zz}\left\{1 - \left[\frac{\tau_a}{a}\exp(E_a/RT)\right]^{(1/b)}\right\} \quad (3)$$

The activation parameters E_a and τ_a were observed to be highly correlated and could unfortunately not be independently determined by the fitting based solely on eq 3. However, A_{zz} was not correlated to E_a and τ_a, and the fitting using eq 3 could therefore be used to determine values of A_{zz}. The activation parameters E_a and τ_a were determined next from an Arrhenius plot of τ_c vs $1/T$, where τ_c was calculated by eq 1 by using the values of A_{zz} determined by the initial fitting by experimental data to eq 3. The results of the fitting procedure are given in **Table 1**, and the temperature dependence of A_{zz}' calculated from these parameters and eq 3 was found to be in good agreement with the experimental data as shown in **Figure 2**. The rotational correlation times, τ_c, that were calculated based on eq 1 and the fitted values of A_{zz} for TEMPOL in the tuna samples increased from 2×10^{-8} s at −15 °C to 2×10^{-7} at −80 °C (**Figure 5**).

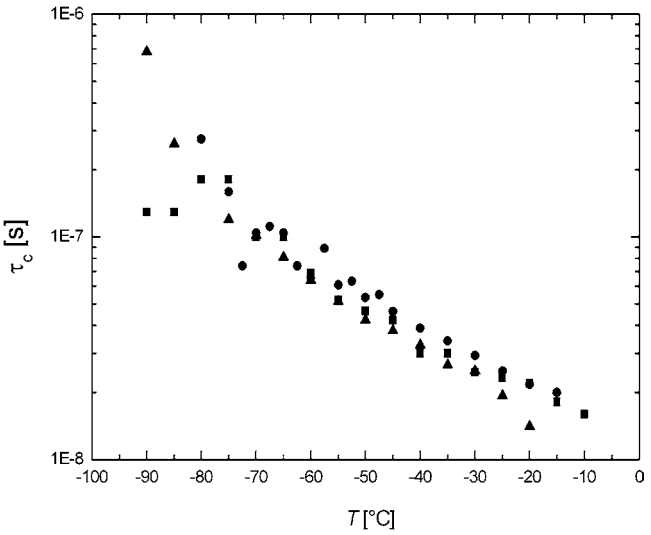

Figure 5. Rotational correlation times, τ_c, for tuna samples. Tuna sample A (■), sample B (●), and sample C (▲).

The magnitude of the rigid limit of the anisotropic hyperfine coupling constant, A_{zz}, is dependent on the polarity of the environment of the spin probe, and values for TEMPOL from 37.5 G in glycerol−water mixtures to 34.3 G in toluene have been reported (*26*, *28*), values which are in agreement with the present estimates (**Table 1**).

It has been suggested, based on DSC experiments, that the water soluble sarcoplasmic protein fraction is the primary class of compounds responsible for forming the glassy state in frozen tuna meat (*7*). For this reason, it was of interest to examine the rotational mobility of TEMPOL as a function of temperature in a solution of sarcoplasmic proteins (**Figure 6**). The major changes in A_{zz}' happened above −55 °C, which is above the glass transition range (from −67 to −58 °C) of freeze concentrated tuna sarcoplasmic proteins (*7*). The temperature dependence of A_{zz}' for TEMPOL in the frozen solution of sarcoplasmic proteins was analyzed by determining activation parameters for the rotational mobility of TEMPOL by the same fitting procedure as used for tuna meat (**Table 1** and **Figure 6**). The sarcoplasmic protein fraction gave significantly higher E_a and lower τ_a for the rotational mobility of TEMPOL than the tuna samples, a finding that is in agreement with a significant role of this protein fraction as glass former.

Control experiments were conducted in order to establish whether the observed low temperature behavior of TEMPOL in tuna meat was caused by small amounts of TEMPOL solutions in the samples and not by TEMPOL absorbed into the meat. The observed A_{zz}' values of TEMPOL in the phthalate

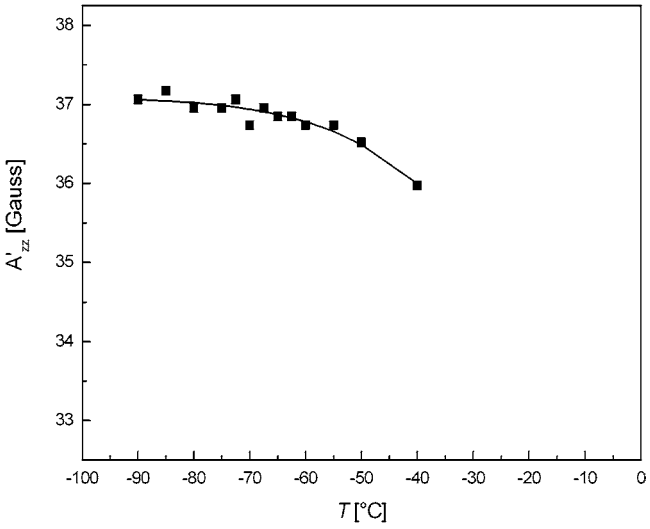

Figure 6. Observed hyperfine coupling constant A_{zz}' as a function of temperature for a 20% w/w sarcoplasmic protein fraction in aqueous TEMPOL solution. The line is the result of the fitting procedure described in the text.

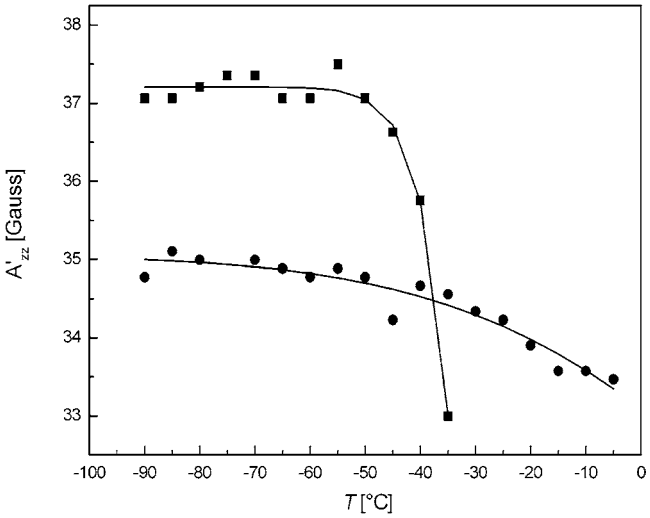

Figure 7. Observed hyperfine coupling constant A_{zz}' as a function of temperature for nonglass forming systems: aqueous TEMPOL–phthalate buffer (■) and unbuffered aqueous TEMPOL (●). The lines are the results of the fitting procedure described in the text.

buffer system were strongly influenced by temperature (**Figure 7**). In the TEMPOL phthalate buffer system, A_{zz}' was independent of the temperature from −90 to −50 °C, thus reflecting the immobilization of TEMPOL. Between −55 and −30 °C, a sharp decrease in A_{zz}' was observed due to local melting of the TEMPOL−salt−ice system. At temperatures above −30 °C, an isotropic three line ESR solution spectrum was observed indicating liquid surroundings of the probe. The temperature dependence of A_{zz}' obtained for a nonbuffered aqueous TEMPOL solution was clearly different from the other systems (**Figure 7**). The values of A_{zz}' were considerably lower and constant up to −50 °C. Above −50 °C, a small decrease in A_{zz}' was observed, and a powder spectrum could be observed at temperatures up to 0 °C, which can be explained as a partial and slow local melting of ice leading to increased mobility of TEMPOL with temperature. The low values of A_{zz}' indicate that TEMPOL is located in nonpolar surroundings in the frozen ice matrix (*26*, *28*). This could be caused by precipitation of TEMPOL during freezing. The activation parameters for the rotational mobility of TEMPOL were determined by the fitting procedure and gave $\log(\tau_a) = -12.7 \pm 0.2$ and $E_a = 26.0 \pm 1.1$ kJ/mol.

The behavior of TEMPOL in both the frozen water and phthalate solution was completely different from the behavior in frozen meat, and it was therefore concluded that the observed behavior of TEMPOL in the marinated tuna meat reflects the behavior of the frozen meat system and not the behavior of the TEMPOL solution that was used for marinating the meat.

Frozen carbohydrate−water mixtures were used as reference systems in order to compare the rotational behavior of TEMPOL in frozen tuna meat to well-studied carbohydrate systems (*18*). The carbohydrate systems were chosen to have different values of T_g' but contain identical amounts of carbohydrates measured as glucose equivalents. The carbohydrate mixtures had values of T_g' ranging from −9 to −47 °C as determined by DSC (all systems) and ADSC (15% sucrose + 20% maltodextrin 5 DE + 15% maltodextrin 9 DE and 23.3% sucrose + 19.3% maltodextrin 5 DE + 7.4% maltodextrin 18.5 DE) (**Table 2**). The rotational mobility of TEMPOL in the carbohydrate mixtures was studied between −10 and −80 °C thus covering temperatures both above and below the glass transitions; however, the temperature dependence of A_{zz}' did not change abruptly at the glass transition temperature, T_g', and the same fitting procedure as for the analysis of the tuna samples was therefore used (**Table 2** and **Figure 8**). The carbohydrate mixtures gave values of E_a from 12.8 to 37.6 kJ/mol, thus covering a larger span than the tuna samples, which is consistent with a large variation in the average molecular weight.

DISCUSSION

The paramagnetic spin probe TEMPOL is easily introduced into tuna meat by diffusion. The behavior of TEMPOL is expected to reflect the behavior of small water soluble solutes in meat, and the temperature dependence of the mobility of TEMPOL can therefore be used as the basis for a discussion of the influence of freezing on the role of deteriorating reactions where mobility of solutes is an important factor (e.g., bimolecular reactions).

The melting of ice domains in the frozen meat was detected by ESR as the presence of a three line isotropic signal in the spectrum of TEMPOL. The melting of ice was observed to take place between −20 and 0 °C, which is in agreement with the range of temperatures for melting of ice as determined by DSC (*7*). The mixed ESR spectra that consisted of powder and isotropic signals did not change with annealing time at each of the studied temperatures indicating that the sample was in thermal equilibrium and that the spectrum was reflecting an equilibrium partition of water between domains of ice and freeze concentrated solution in the frozen tuna. The use of spin probes and ESR detection appears to be well-suited to characterize the gradual freeze concentration and formation of ice that take place over a temperature range. This supplements the DSC technique, where the detection of ice melting is easily distorted by the finite temperature scanning rate and the relative large amounts of heat that are transferred (*7*).

Below −20 °C, only ESR powder spectra were observed indicating a very low mobility of TEMPOL. The mobility of TEMPOL in frozen tuna was studied at temperatures above and in the T_g' zone where the glass transition takes place. The temperature corresponding to the melting of the glassy state in tuna meat has been determined by DSC $T_g' = -74$ °C (*7*); however, no abrupt changes in the temperature dependence of the mobility of the spin probe in the frozen tuna at T_g' were

Table 2. Glass Transition Temperatures, Rigid Limit Hyperfine Coupling Constants, and Arrhenius Activation Parameters for the Rotational Mobility of TEMPOL in Frozen Carbohydrate Systems with 50% Water[a]

wt % of carbohydrates (symbol)[b]	T_g' (°C)	A_{zz} (Gauss)	E_a (kJ/mol)	log(τ_a)
50% sucrose (◆, - · · -)	–47[c]	38.08 ± 0.04	37.6 ± 6.3	–15.41 ± 1.43
50% maltodextrin 5 DE (■, —)	–9[c]	37.92 ± 0.18	12.8 ± 0.5	–10.30 ± 0.11
50% maltodextrin 9 DE (●, - - -)	–13[c]	37.54 ± 0.05	17.1 ± 0.5	–11.02 ± 0.12
50% maltodextrin 18.5 DE (▲, · · ·)	–20[c]	37.44 ± 0.03	22.2 ± 0.9	–12.00 ± 0.19
3% sucrose + 44% maltodextrin 5 DE + 3% maltodextrin 9 DE (□, —)	–12[c]	37.85 ± 0.18	13.0 ± 0.5	–10.29 ± 0.11
15% sucrose + 20% maltodextrin 5 DE + 15% maltodextrin 9 DE (○, - - -)	–20[c,d]	37.41 ± 0.06	24.1 ± 1.8	–12.33 ± 0.39
23.3% sucrose + 19.3% maltodextrin 5 DE + 7.4% maltodextrin 18.5 DE (△, · · ·)	–31[c,d]	37.47 ± 0.04	27.5 ± 1.7	–13.02 ± 0.37

[a] Errors are reported as the SD. [b] The symbol and line refer to **Figure 8**. [c] Measured with DSC. [d] Measured with ADSC.

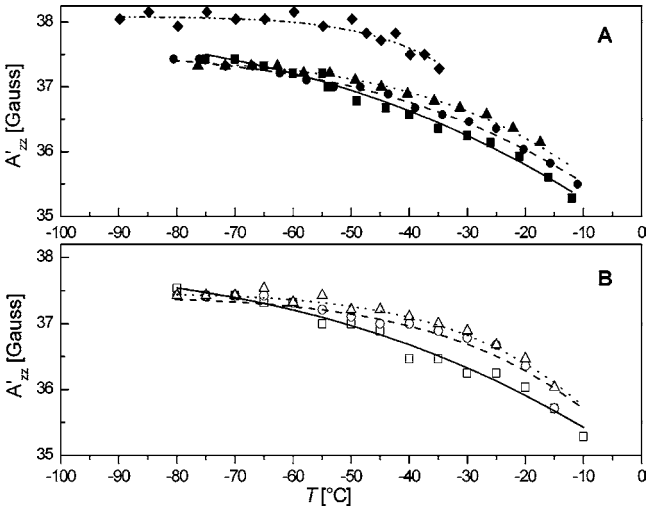

Figure 8. Observed hyperfine coupling constant A_{zz}' for a 2.3 mM TEMPOL solution as a function of temperature for carbohydrate–water mixtures. (**A**) 50% maltodextrin 5 DE (■, —), 50% maltodextrin 9 DE (●, – – –), 50% maltodextrin 18.5 DE (▲, · · ·), and 50% sucrose (◆, - · · -). (**B**) 3% sucrose + 44% maltodextrin 5 DE + 3% maltodextrin 9 DE (□, —), 15% sucrose + 20% maltodextrin 5 DE + 15% maltodextrin 9 DE (○, – – –), and 23.3% sucrose + 19.3% maltodextrin 5 DE + 7.4% maltodextrin 18.5 DE (△, · · ·). The lines are the results of the fitting procedure described in the text.

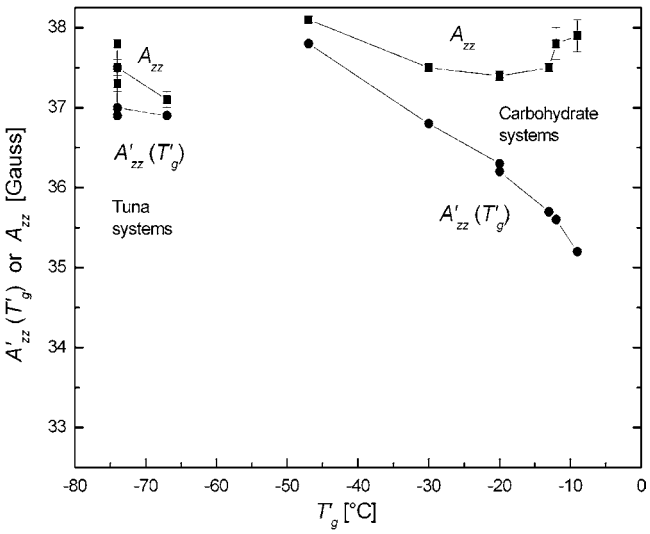

Figure 9. Observed hyperfine coupling constant at T_g', $A_{zz}'(T_g')$, as a function of the maximally freeze-concentrated glass transition temperature, T_g' (■). The rigid limiting value, A_{zz}, as a function of T_g' (●).

observed by ESR (**Figure 2**). Similar results were also observed for sarcoplasmic proteins where the glass transition temperature as determined by DSC is $T_g' = -67$ °C (*7*). The lack of abrupt changes in the observed mobility of the spin probe at the glass transition temperatures could be due to the low mobility of the spin probe in the vicinity of the glass transition temperature, which is close to the limit of detection as changes in powder spectra when observed by conventional CW-ESR experiments. A further decrease in the mobility of the spin probe would not be observed since it would be too slow to be detected.

Several studies (*17*, *19*−*21*, *27*, *29*−*31*) have suggested an effect of the glass transition temperature on molecular mobility in glassy systems. The rotational spin probe mobility measurements conducted by conventional ESR and saturation transfer ESR (ST-ESR) (*20*, *21*, *27*, *29*−*31*) gave rotational correlation times in the range of 10^2−10^{-9} s, and the rotational correlation time at T_g between 10^{-2} and 10^{-5} s. In the present study, the analysis of the temperature dependence of the powder spectra gave values of τ_c in the range of 2×10^{-8} to 2×10^{-7} s as calculated by eq 1. This is several orders of magnitude faster than the values found for the rotational mobility of TEMPOL in glassy carbohydrate systems by using the ST-ESR technique, and it has been argued that correlation times in this range stem from vibrational motion of the immobilized spin probe and are too fast to be caused by complete rotational motions in glassy systems (*18*, *32*). The spin probe and other molecules of similar size may thus be trapped in the glass where they move but do not fully rotate.

It has been reported that an abrupt change in A_{zz}' at the glass transition temperature coincided with the T_g as measured by DSC for dry pea seed axes (*17*) and various organic glasses (*19*). In these studies, the mobility parameter, A_{zz}', was measured by conventional ESR below and above the glass transition temperature, T_g (DSC). To assess the impact of the glassy state on mobility of TEMPOL, different glassy carbohydrate systems were examined. However, in the present study, abrupt changes in the temperature dependency of the hyperfine coupling constant were not observed for the carbohydrate systems where the mobility of TEMPOL could be studied both below and above the respective glass transition temperatures.

The rigid limit hyperfine coupling constants, A_{zz}, were found to have the same value for tuna and carbohydrate samples reflecting that the environment of TEMPOL had the same polarity in all samples (**Tables 1** and **2**). The value of the observed hyperfine coupling constant at the maximally freeze concentrated glass transition temperature, $A_{zz}'(T_g')$, which can be used as a measure of the mobility of TEMPOL at T_g', was found to depend on the type of sample (**Figure 9**). The systems with a low T_g' (including the tuna samples) had values of A_{zz}'-(T_g') that were close to A_{zz}, and $A_{zz}'(T_g')$ can therefore not be used to give information about the mobility of TEMPOL at T_g' for these samples. However, the carbohydrate systems gave an almost linear decrease in $A_{zz}'(T_g')$ as a function of T_g', **Figure 9**, indicating increasing mobility of TEMPOL with increasing

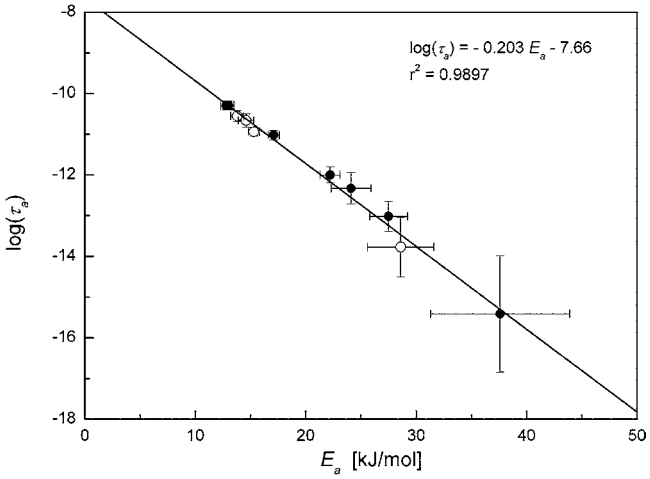

Figure 10. Correlation between the Arrhenius preexponential factors, τ_a, and the activation energies, E_a, for tuna (○) and carbohydrate samples (●).

T_g'. A similar relationship of decreasing rotational correlation times at T_g, $\tau_c(T_g)$, with increasing T_g has been observed (*18*, *31*). It has been suggested that the molecular packing density decreases upon increasing molecular weight of the glass forming molecules, which leads to an increase in the free volume available for rotational motions of the spin probe (*18*, *27*). Thus, it is likely that the observed mobility of TEMPOL is decoupled from the mobility of the glass forming components in the tuna and carbohydrate systems.

The logarithms of the preexponential factors, τ_a, obtained by the analysis of the correlation times by the Arrhenius equation, are linearly correlated to the corresponding activation energies E_a for all of the studied systems (**Figure 10**). The linear correlation between $\log(\tau_a)$ and E_a indicates that the observed mobility of TEMPOL is subjected to enthalpy−entropy compensation effects, which arise when $\Delta H^{\ddagger} = \alpha + \beta\Delta S^{\ddagger}$ for a series of similar systems, where $\Delta H^{\ddagger}$ and $\Delta S^{\ddagger}$ are the enthalpy and entropy of activation, respectively, of the motion of the spin probe (*33*, *34*). Such linear correlations between enthalpy and entropy arise when the observed reaction (mobility in the present case) is thermodynamically strongly coupled to the surroundings. The observed linearity was shown to arise from chemical and physical effects and not from statistical effects by plotting $\Delta G^{\ddagger}$ as a function of $\Delta H^{\ddagger}$, where $\Delta H^{\ddagger}$ and $\Delta G^{\ddagger}$ were derived from the activation parameters in **Tables 1** and **2**. The plot gave a linear correlation between $\Delta H^{\ddagger}$ and $\Delta G^{\ddagger}$ for all of the samples, indicating that the linearity between $\log(\tau_a)$ and E_a in **Figure 10** is caused by chemical and physical effects (*35*). The strong linear correlation between $\log(\tau_a)$ and E_a suggests that the mechanism of the motion of TEMPOL is the same for all of the frozen samples. It is noteworthy that the tuna samples do not deviate from the correlation, indicating an identical type of motion of TEMPOL in the carbohydrate mixtures and the tuna samples despite the differing natures of the frozen samples. The frozen tuna samples are highly heterogeneous systems as compared to the frozen carbohydrate samples. The observed mobility of TEMPOL in the frozen meat and the carbohydrate mixtures is therefore very likely probing the dynamics of the nearest surrounding molecules of the probe in the frozen matrix, which are affected by the mobility of the glass forming macromolecules. It is possible that the Arrhenius activation parameters for the mobility of the probe reflect the strength of the frozen matrix; however, further studies are needed in order to test this hypothesis.

In conclusion, it has been shown that the ESR spin probe technique can be used to monitor molecular mobility in frozen food systems. For the studied food systems, it is seen that there are no abrupt decreases in molecular mobility at the maximally freeze concentrated glass transition temperature. Moreover, the mobility of nonglass forming solutes such as the spin probe is decoupled from the mobility of the glass forming components.

ACKNOWLEDGMENT

Lis B. Meyer is thanked for skillful technical assistance.

LITERATURE CITED

(1) Bjerkeng, B.; Johnsen, G. Frozen Storage Quality of Rainbow Trout (Oncorhynchus mykiss) as Affected by Oxygen, Illumination, and Fillet Pigment. *J. Food Sci.* **1995**, *60* (2), 284−288.

(2) Jensen, C.; Birk, E.; Jokumsen, A.; Skibsted, L. H.; Bertelsen, G. Effect of dietary levels of fat, α-tocopherol and astaxanthin on colour and lipid oxidation during storage of frozen rainbow trout (Oncorhynchus mykiss) and during chill storage of smoked trout. *Z. Lebensm. Unters. Forsch. A* **1998**, *207*, 189−196.

(3) Brake, N. C.; Fennema, O. R. Lipolysis and Lipid Oxidation in Frozen Minced Mackerel as Related to Tg′, Molecular Diffusion, and Presence of Gelatin. *J. Food Sci.* **1999**, *64* (1), 25−32.

(4) Ablett, S.; Izzard, M. J.; Lillford, P. J. Differential Scanning Calorimetry Study of Frozen Sucrose and Glycerol Solutions. *J. Chem. Soc., Faraday Trans.* **1992**, *88* (6), 789−794.

(5) Roos, Y.; Karel, M. Water and Molecular Weight Effects on Glass Transitions in amorphous Carbohydrates and Carbohydrate Solutions. *J. Food Sci.* **1991**, *56* (6), 1676−1681.

(6) Bai, Y.; Rahman, M. S.; Perea, C. O.; Smith, B.; Melton, L. D. State diagram of apple slices: glass transition and freezing curves. *Food Res. Int.* **2001**, *34*, 89−95.

(7) Orlien, V.; Risbo, J.; Andersen, M. L.; Skibsted, L. H. The Question of High or Low-temperature Glass Transition in Frozen Fish. Construction of the Supplemented State Diagram for Tuna Muscle by Differential Scanning Calorimetry. *J. Agric. Food Chem.* **2003**, *51*, 211−217.

(8) Roos, Y.; Karel, M.; Kokini, J. L. Glass Transitions in Low Moisture and Frozen Foods: Effects on Shelf Life and Quality. *Food Technol.* **1996**, 95−108.

(9) Goff, H. D. Low-temperature stability and the glassy state of frozen foods. *Food Res. Int.* **1992**, *25*, 317−325.

(10) Simatos, D.; Blond, G. DSC studies and stability of frozen foods. In *Water Relationships in Foods*; Levine, H., Slade, L., Eds.; Plenum Press: New York, 1991; pp 139−155.

(11) Reid, D. Optimizing the Quality of Frozen Foods. *Food Technol.* **1990**, *78*, 80−82.

(12) Levine, H.; Slade, L. Principles of "cryostabilization" technology from structure/property relationships of carbohydrate/water systems—a review. *Cryo-Lett.* **1988**, *9*, 21−63.

(13) Andersen, A. B. Chemical stability of food systems in the vicinity of the glass transition. Ph.D. Thesis, The Royal Veterinary and Agricultural University, Frederiksberg, Denmark, 2000.

(14) Le Meste, M.; Champion, D.; Roudaut, G.; Blond, G.; Simatos, D. Glass Transition and Food Technology: A Critical Appraisal. *J. Food Sci.* **2002**, *67* (7), 2444−2458.

(15) Champion, D.; Le Meste, M.; Simatos, D. Towards an improved understanding of glass transition and relaxations in foods: molecular mobility in the glass transition range. *Trends Food Sci. Technol.* **2000**, *11*, 41−55.

(16) Contreras-Lopez, E.; Champion, D.; Hervet, H.; Blond, G.; Le Meste, M. Rotational and Translational Mobility of Small Molecules in Sucrose plus Polysaccharide Solutions. *J. Agric. Food Chem.* **2000**, *48*, 1009−1015.

(17) Buitink, J.; Dzuba, S. A.; Hoekstra, F. A.; Tsvetkov, Y. D. Pulsed EPR Spin-Probe Study of Intracellular Glasses in Seed and Pollen. *J. Magn. Reson.* **2000**, *142*, 364−368.

(18) van den Dries, I. J.; van Dusschoten, D.; Hemminga, M. A.; van der Linden, E. Effects of Water Content and Molecular Weight on Spin Probe and Water Mobility in Malto-oligomer Glasses. *J. Phys. Chem. B* **2000**, *104*, 10126−10132.
(19) Paschenko, S. V.; Toropov, Y. V.; Dzuba, S. A.; Tsvetkov, Y. D.; Vorobiev, A. Kh. Temperature dependence of amplitudes of libration motion of guest spin-probe molecules in organic glasses. *J. Chem. Phys.* **1999**, *110* (16), 8150−8154.
(20) van den Dries, I. J.; de Jager, P. A.; Hemminga, M. A. Sensitivity of saturation Transfer Electron Spin Resonance Extended to Extremely Slow Mobility in Glassy Materials. *J. Magn. Reson.* **1998**, *131*, 241−247.
(21) Roozen, M. J. G. W.; Hemminga, M. A. Molecular Motion in Sucrose-Water Mixtures in the Liquid and Glassy State As Studied by Spin Probe ESR. *J. Phys. Chem.* **1990**, *94*, 7326−7329.
(22) Hansen, E.; Andersen, M. L.; Skibsted, L. H. Mobility of solutes in frozen pork studied by electron spin resonance spectroscopy: evidence for two phase transition temperatures. *Meat Sci.* **2003**, *63*, 63−67.
(23) Rahman, S. F.; Kasapis, S.; Guizani, N.; Al-Amri, O. S. State diagram of tuna meat: freezing curve and glass transition. *J. Food Eng.* **2003**, *57*, 321−326.
(24) Brake, N. C.; Fennema, O. R. Glass transition values of muscle tissue. *J. Food Sci.* **1999**, *64*, 10−15.
(25) Freed, J. Theory of slow tumbling ESR spectra for nitroxides. In *Spin Labeling. Theory and Applications*; Berliner, L. J., Ed.; Academic Press: New York, 1976; Chapter 3, pp 53−132.
(26) Marsh, D.; Kurad, D.; Livshits, V. A. High-field electron spin resonance of spin labels in membranes. *Chem. Phys. Lipids* **2002**, *116*, 93−114.
(27) Roozen, M. J. G. W.; Hemminga, M. A.; Walstra, P. Molecular motion in glassy water-malto-oligosaccharide (maltodextrin) mixtures as studied by conventional and saturation-transfer spin-probe esr spectroscopy. *Carbohydr. Res.* **1991**, *215*, 229−237.
(28) Ondar, M. A.; Grinberg, O Ya.; Dubinskii, A. A.; Lebedev, Ya. S. Study of the effect of the medium on the magnetic-resonance parameters of nitroxyl radicals by high-resolution EPR spectroscopy. *Sov. J. Chem. Phys.* **1985**, *3*, 781−792.
(29) van den Berg, C.; van den Dries, I.; Hemminga, M. A. Molecular Mobilities around the Glass Transition in Sugar-Water systems. *Magn. Reson. Food Sci.* **1995**, 93−101.
(30) Hemminga, M. A.; van den Dries, I. J.; Magusin, P. C. M. M.; van den Berg, C. Molecular Mobility in food Components as Studied by Magnetic Resonance Spectroscopy. In *Water Management in the Design and Distribution of Quality Foods*; ISOPOW 7; Roos, Y. H., Leslie, R. B., Lillford, P. J., Eds.; Technomic Press: Lancaster, PA, 1999; pp 255−265.
(31) Buitink, J.; van den Dries, I. J.; Hoekstra, F. A.; Alberda, M.; Hemminga, M. A. High Critical Temperature above Tg May Contribute to the Stability of Biological Systems. *Biophys. J.* **2000**, *79*, 1119−1128.
(32) Dzuba, S. A. Librational motion of guest spin probe molecules in glassy media. *Phys. Lett. A* **1996**, *213*, 77−84.
(33) Grunwald, E.; Steel, C. Solvent reorganization and thermodynamic enthalpy−entropy compensation. *J. Am. Chem. Soc.* **1995**, *117*, 5687−5692.
(34) Liu, L.; Guo, Q.-X. Isokinetic relationship, isoequilibrium relationship, and enthalpy−entropy compensation. *Chem. Rev.* **2001**, *101*, 673−695.
(35) Krug, R. R.; Hunter, W. G.; Grieger, R. A. Enthalpy−Entropy Compensation. 2. Separation of the Chemical from the Statistical Effect. *J. Phys. Chem.* **1976**, *80*, 2341−2351.

Received for review August 18, 2003. Revised manuscript received February 2, 2004. Accepted February 13, 2004. The support of Helsinki University, Finland, to S.J. as an exchange student of food science, is gratefully acknowledged. This research was sponsored by the FØTEK 3 program through LMC−Centre for Advanced Food Studies as a part of the project "Molecular Mobility in Foods undergoing Phase Transitions".

JF034931G